Journal of Organometallic Chemistry 882 (2019) 10–17

Contents lists available at ScienceDirect

Journal of Organometallic Chemistry

journal homepage: www.elsevier.com/locate/jorganchem

Synthesis, characterization, and photophysical properties of bismetalated platinum complexes with benzothiophene ligands

Craig M. Anderson [a, *], Claudio Mastrocinque [a], Matthew W. Greenberg [a], Ian C. McClellan [a], Leila Duman [a], Nathaniel Oh [a], Francesco Mastrocinque [a], Michael Pizzuto [a], Kaylynn Tran [a], Joseph M. Tanski [b]

[a] Department of Chemistry, Bard College, 30 Campus Road, Annandale-on-Hudson, NY, 12504, USA
[b] Department of Chemistry, Vassar College, Poughkeepsie, NY, 12604, USA

ARTICLE INFO

Article history:
Received 16 November 2018
Received in revised form
13 December 2018
Accepted 13 December 2018
Available online 24 December 2018

This manuscript is dedicated to Professor Richard Puddephatt on the occasion of his 75th birthday. We greatly appreciate his excellent mentorship over the last several decades.

Keywords:
C–H activation
Phosphorescence
Benzothiophene
TD-DFT
Cyclometalation

ABSTRACT

Benzothiophene-based ligands containing quinoline or pyridine moieties were synthesized through Suzuki Coupling reactions and subsequently reacted with the binuclear Platinum compound, [Pt_2Me_4 (μ-SMe_2)$_2$], **PtA**, in order to study chelate-assisted C–H activation. The preparation and characterization of C^N cyclometalated products, including η^2 intermediates, monometalated, and bismetalated species, are reported. The photophysical properties of the complexes were studied and compared to TD-DFT computational results.

© 2018 Published by Elsevier B.V.

1. Introduction

Cyclometalated and orthometalated complexes have many practical applications in material science and as artificial photosynthetic devices [1–8]. Many of these cyclometalated species, when utilizing methyl platinum precursors, are formed by C–H activation reactions followed immediately by reductive elimination of methane [9–12]. Ring size is an interesting variable to consider when studying cyclometalated species, as ring size may vary physical and chemical properties [13–22]. Thus, synthesizing different ring sizes by varying ligand architecture may allow for subtle or gross changes in the physical and/or chemical properties. Appropriately designed ligands are therefore necessary in order to guide the regiochemistry of the initial C–H oxidative addition.

Due to the heterocyclic nature of benzothiophene, it is a useful material in the production of biologically active drugs and examples of benzothiophene moieties in pharmaceuticals and dyes exist [23–26]. Benzothiophene has additional aromatic conjugation than its related species, thiophene, which is well-known for its interesting photophysical behavior and has been used in many applications in dye-sensitized solar cells and photodetectors [27].

Bismetallated complexes are somewhat more rare than their monometalated counterparts and might be expected to be more rigid than the monometlated analogues [9,28–30]. This additional rigidity may aid in augmenting the compounds photophysical properties including longer excited state lifetimes [31,32]. Thus, we report and describe the synthesis and photophysical properties of bis-cyclometalated platinum (II) compounds with chelating N^C ligands that contain a benzothiophene moiety.

* Corresponding author.
E-mail address: canderso@bard.edu (C.M. Anderson).

https://doi.org/10.1016/j.jorganchem.2018.12.010
0022-328X/© 2018 Published by Elsevier B.V.

Table 1
Structures for ligand, intermediates, and N^C metallacycles.

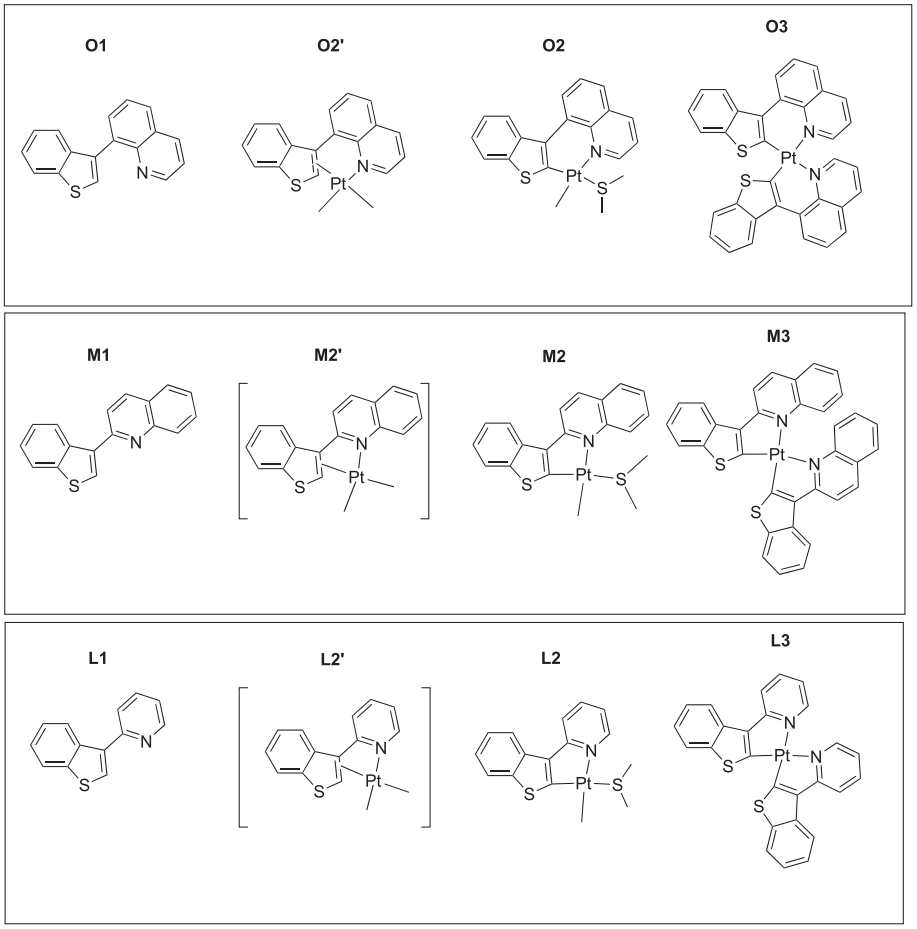

2. Results and discussion

Ligand **O1** (Table 1 and Scheme 1) was synthesized by a Suzuki-type coupling reaction and its structure is analogous to a thiophene-derivative ligand reported by Tan et al. [33], with a benzothiophene in place of thiophene. The ligand was characterized by NMR spectroscopy and X-ray diffraction (XRD). The structure of **O1** (Fig. 1), obtained by XRD, clearly shows the expected product of the coupled benzothiophene and quinolone moieties. Upon allowing the chelate ligand **O1** to react with **PtA** a new compound was formed, **O2′**, as a result of substitution of **O1** for the two labile dimethylsulfide ligands. **O2′** was isolated and the proposed structure has a chelate ligand which includes the coordinated nitrogen and an η^2 moiety originating from the benzothiophenene [34]. The species was characterized by its proton NMR spectrum. For example, the proton closest to the η^2 bond of the intermediate is more upfield and shielded than its aromatic ligand counterpart because of its interaction with the Pt, therefore appearing at midrange in the spectrum at 6.22 ppm with platinum satellites with couplings of 51 Hz. Two distinct methyl resonances are observed and appear as singlets exhibiting platinum satellites peaks characteristic of Pt coordination. A peak representing one of the methyls appears at 1.10 ppm with a coupling constant of 88 Hz. The peak representing the other methyl group appears further upfield at −0.41 ppm with coupling constant of 81 Hz. **O2′**, was characterized by carbon-13 NMR, showing the appropriate 17

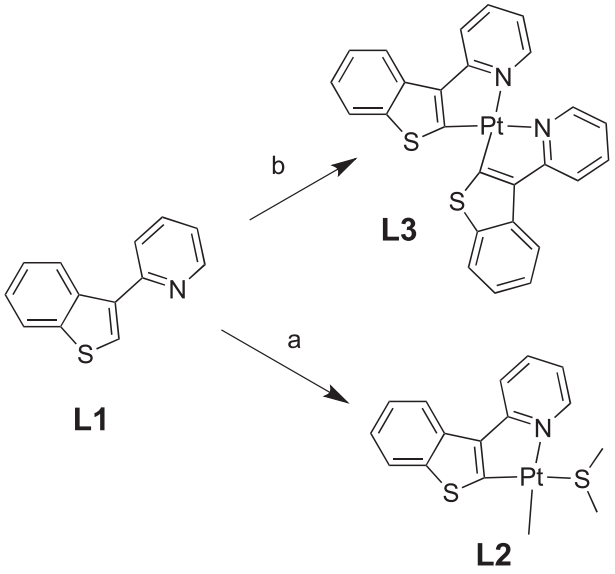

Scheme 1. Reaction of ligand **L1** with **PtA** to form metalated species. a) 2 equiv. of **L1**, stirred in toluene 2 h at room temp. followed by heating to 60 for 1 h; b) **L1** with **PtA** heated at 80C for 5 h followed by 1 h irradiation with 450 nm light.

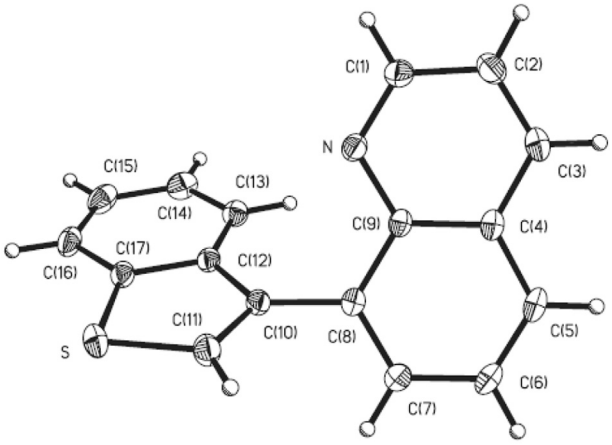

Fig. 1. ORTEP of Compound **O1** (50% probability thermal ellipsoids). Selected bonds lengths (Å) and angles (°):C7–C8: 1.3781 (16); C8–C9: 1.4285 (15); C8–C10: 1.4818 (15); S–C11 1.7283 (13); S–C17 1.7376 (13); N–C1 1.3193 (15); N–C9 1.3708 (14); C11–S–C17 91.38 (6); C1–N–C9 117.7 (1); C11–C10–C8 123.4 (1); C12–C10–C8 124.7 (1); C7–C8–C10 120.3 (1); C9–C8–C10 120.70 (10).

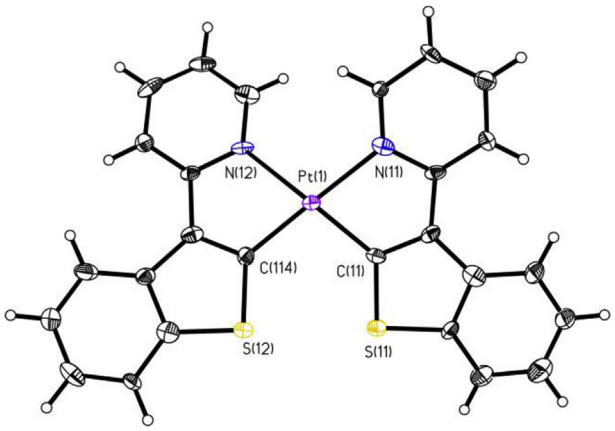

Fig. 2. ORTEP of Compound **L3** (50% probability thermal ellipsoids). Selected bonds lengths (Å) and angles (°): Pt–N (11): 2.133 (7); Pt1–N12: 2.116 (7); Pt–C (11): 1.964 (9); Pt1–C114 1.978 (9); C11–Pt1–C114; 101.5 (4); C11–Pt1–N11: 78.0 (3); C114–Pt1–N11: 171.0 (4); C11–Pt1–N12: 168.7 (3); C114–Pt1–N12: 78.0 (3); N11–Pt1–N12: 104.3 (3).

carbon peaks in the ^{13}C NMR including the two distinct methyl peaks upfield. **O2,** with a six-membered platinacycle was synthesized directly from **O1** and **PtA** when a solution of the two compounds were refluxed in toluene. This resulted in pure **O2**, whereas when **O2'** was subjected to the same conditions, a clean reaction was not observed. **O3** was not obtained by thermal or photochemical reactions (Table 1).

The reactions of the two ligands **L1** and **M1** with **PtA** differed from the reaction of **O1** with **PtA**. The η^2 intermediate was not observed in either case prior to the formation of the five-membered platinacycles. However, the monometalated intermediate **L2** was obtained in pure form, but the monometalated **M2** was not. Attempts at **M2** gave only mixtures of species of which **M2** was speculated to be one of them, but **M2** could not be extracted or got in purified form without decomposition of the products. Presumably the formation of these metalacycle go through an η^2 intermediate as in the case of **O2'**; however, the reaction to form the five-membered rings for **L2** and **M2** must be faster, compared to the six-membered ring for **O2**, thus the η^2 intermediate is too short-lived to be observed, which is reasonable considering that five-membered rings predominate in the literature [35,36].

The proton NMR spectra were invaluable in the characterization of the compounds.

For example, **L2** has one platinum methyl and one DMS resonance present at the appropriate chemical shifts (1.23 and 2.51 ppm, respectively) and coupling constants (79 Hz and 30 Hz, respectively) for platinum (II) monometalated species [37]. When the synthesis of bismetalaed species were attempted using standard thermal techniques (whether beginning with **PTA** or the monometalated species) and when monitoring the reaction while heating, mixtures of monometalated species, species tentatively assigned as κ^1/κ^2 species [38], and/or mixtures of bismetalated species were observed (Table 1), somewhat similar to that observed in the attempted syntheses of **M2**. However, pure bismetalated species were isolated in each case using a photochemical technique adapted from Julia et al. [39]. The ligand and metal precursor were mixed and heated for several hours followed by irradiation with blue light for an additional duration of time. This afforded a crude material, which when purified by column chromatography resulted in isolation of a bismetalated species in modest yields. **M3** and **L3** were characterized by multi-nuclear NMR and HRMS, while **L3** (Fig. 2) was characterized by X-ray diffraction techniques (XRD).

The proton spectra of the bismetalated species showed the absence of the platinum-methyl group as expected with the second metalation and thus only aromatic resonances remained (See SI for NMR spectra). For example, **M3** showed the expected 10 resonances (Fig. 3) and **L3** the expected 8 aromatic resonances. Attempts at synthesizing **O3** were unsuccessful. Insoluble, uncharacterized material was formed.

The structure of L3 (Fig. 2) has a square planar platinum (II) metal center with two C^N chelate ligands. The pyridine rings of each ligand are cis to each other rendering the expected trans geometry of each carbon donor to each nitrogen donor of the C^N chelate ligand, thus avoiding trans carbons due to their high trans influence. L3 adopts a distorted square planar geometry in the solid state, with a significant dihedral angle between the two planes defined by Pt (1)-N (12)-C (114) and Pt (1)-N (11)-C (11) (Fig. 2). For the two nearly identical molecules of L3 in the asymmetric unit, this angle is 16.04° and 15.47° for Pt (1) and Pt (2) respectively. While this distortion from an ideal square planar geometry could simply reflect crystal packing effects in the solid state, the DFT optimized geometry of a single gas phase molecule of L3 shows a chelate dihedral angle of 16.10° (Figure SI1). This structure was confirmed to represent an energetic minimum by vibrational analysis, and was found even when a square planar structure was used as the input geometry. The good correspondence between the

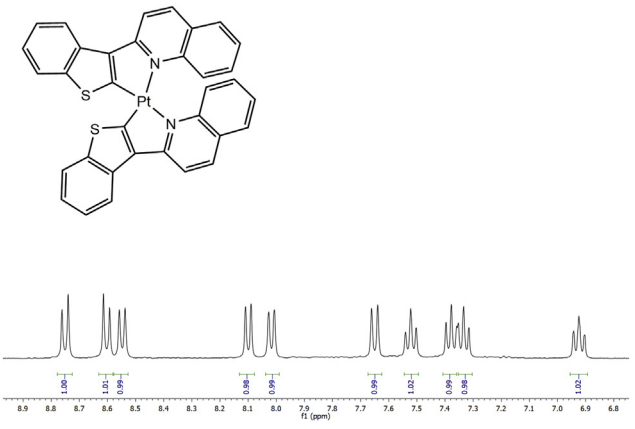

Fig. 3. Proton NMR spectrum (400 MHz) of **M3** in $(CD_3)_2SO$.

computational results found in the gas phase and the experimental results found in the solid state strongly suggests that this geometrical distortion from an ideal square planar geometry is a result of the steric profile of the benzothiophene chelate used here.

3. Photophysical measurements and computational results

The isolated compounds, most importantly the target bismelatated species, were characterized by UV/vis and emission spectroscopy. Data can be found in Table 2. The ligands have large absorbance bands for their lowest energy band at around 300 nm. **O1** emits with a red-shift of around 115 nm, while **O2's** emission is red-shifted twice that amount. **L2** absorbs just above 400 nm and emits in the orange region with two shoulders. The target bismetalated compounds have their lowest energy absorbance in the visible region and they have extinction coefficients in the 10^3-10^4 range (Table 2). Their emission spectra show peaks that are red-shifted 150–200 nm (Fig. 4). **L3** has a well-defined shoulder at lower energy that has a longer lifetime than the large, primary peak, perhaps due to excimer formation [40]. Excited state lifetimes for **L3** and **M3** are greater than a microsecond and their quantum yields are modest at 2.3 and 3.0% for **L3** and **M3**, respectively. The data lead us to conclude that their emission is phosphorescence from MLCT states.

Time-Dependent Density Functional Theory (TD-DFT) calculations were run on **L3** to interrogate the nature of the observed electronic transitions in the UV/vis (Figure SI2). The experimental UV–vis spectrum and the TD-DFT calculated UV–vis spectrum obtained by optimizing the first 30 excited states show a good qualitative agreement to the experimental spectrum of **L3** as is seen in Fig. 5. Examination of the TD-DFT Natural Transition Orbitals [41] associated with the high oscillator strength transitions, which correspond to major peaks in the experimental spectra of **L3**, allowed characterization of the nature of these transitions. The observed hole and particle NTOs of the lower energy peaks with large oscillator strengths which correspond to experimentally observed absorption features are consistent with mixed Metal to Ligand Charge Transfer/Intraligand Charge Transfer (MLCT/ILCT) [42–44] character of these transitions with the hole wavefunction primarily localized on the electron rich thiophene moiety and platinum atom and the particle wavefunction localized primarily on the pyridine moiety (Fig. 6). Consequently, the lowering of the lowest unoccupied π^* orbitals by the increased conjugation of quinoline compared to pyridine should result in the appearance of redshifted absorption features in **M3** as compared to **L3**, which is observed experimentally.

4. Concluding remarks

The reactions of $[Pt_2Me_4(\mu\text{-}SMe_2)_2]$ with the quinoline or pyridine functionalized benzothiophene ligands highlight several interesting patterns related to the effect of ligand structure and composition on the selective chelate assisted C–H activation process. In all cases, the selected C–H bond at the 2-position of the thiophene moiety successfully underwent a regioselective reaction by what is generally proposed to be a concerted oxidative addition mechanism to produce a putative Pt (IV) intermediate, which quickly reductive eliminated methane. Five-membered metalacycles are formed with pyridine-derived ligands and a six-membered ring with the quinolone moiety and an η^2 intermediate is observed in the latter case. The bismetalated species was then formed by another such series of reactions, however a

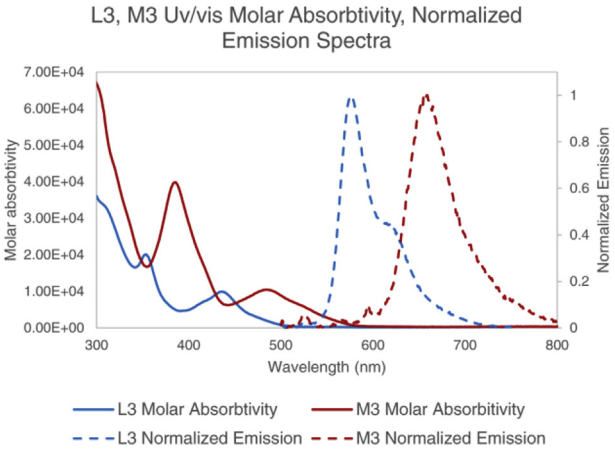

Fig. 4. Emission and Uv/vis Spectra for the bismetalated species **L3** and **M3**.

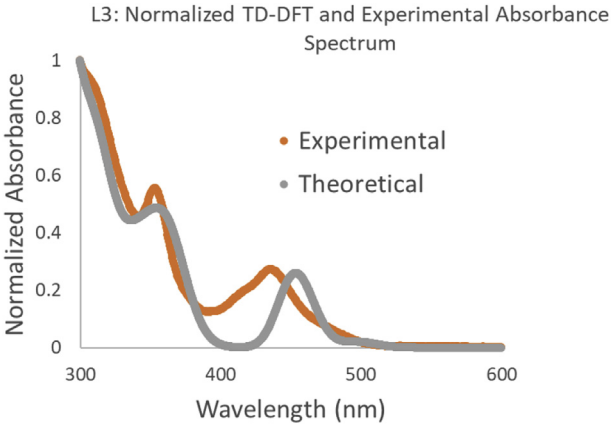

Fig. 5. Comparison of experimental and TD-DFT calculated normalized absorbance spectrum. The theoretical absorbance spectrum is visualized by the convolution of the discrete eigenspectrum with gaussian functions of 25 nm half-width.

Table 2
Photophysical data.

Complex	Absorption λ_{max}/nm (ε/$M^{-1}cm^{-1}$)	Emission λ_{max}/nm	Lifetime ns (χ2)
L1	248 (7620), 282 (7350)	353	0.2 (1.142)[a]
L2	331 (5460), 368 (2330), 412 (1670)	541, 618, 677	887 (1.080)[a]
L3	353 (15500), 436 (9900)	577, 620	805 (1.069)[b] (577) 1470 (1.070)[b] (620)
M1	236 (51700), 312 (14300), 329 (13700)	384	–
M3	385 (42800), 484 (11800)	660	1700 (0.9739)[b]
O1	292 (8244), 301 (8673)	416	58 (1.137)[c]
O2′	398 (919)	660	347 (1.032)[a]
O2	357 (5011), 460 (2930)	656	457 (1.076)[a]

?$_{excitation}$ = [a] 405 nm, [b] 450 nm, [c] 365 nm.

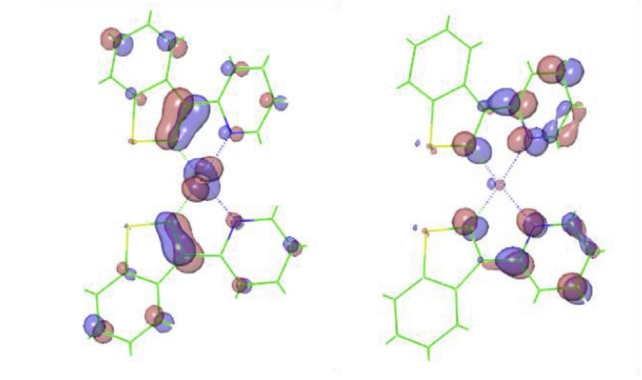

Fig. 6. Calculated Hole (left) and Particle (right) wavefunctions for the high oscillator strength calculated electronic transition at 453 nm.

photochemical process was necessary to obtain a viable product. The bismetalated species had more pronounced photophysical properties, including longer excited state lifetimes, than the monometalated analogue. This may be due to the planarity of the ligands and the rigidity of the bis-etalated species, but tempered due to the somewhat large dihedral angle between ligands as observed in the structure of **L3**. We are currently testing these compounds on a variety of catalytic reactions.

5. Experimental section

5.1. General

The solvents and reagents were purchased from Sigma Aldrich unless otherwise noted. K_2PtCl_4 was purchased from the Pressure Chemical Company. NMR spectra were recorded at Bard College using Varian MR-400 MHz spectrometer (^{1}H, 400 MHz; ^{13}C, 100.6 MHz) and referenced to $SiMe_4$ (^{1}H, ^{13}C). Shifts are given in ppm and coupling constant *J* values in Hz. Abbreviations used: s = singlet; d = doublet; t = triplet; m = multiplet. Electrospray mass spectra were performed at Vassar College using an LC/MSD-TOF spectrometer.

5.2. Computational details

Calculations were carried out using TD-DFT and DFT implemented in the Jaguar 9.1 suite of *ab initio* quantum chemistry programs. Geometry optimizations were performed with the B3LYP functional using the LACVP** basis set [45]. In all cases, the geometries were confirmed to be energetic minima by vibrational analysis. In the case of the TD-DFT calculations, the UV/Vis absorbance spectrum was simulated by optimization of the first 30 excited states and the use of a Poisson-Boltzmann implicit solvation model of dichloromethane to improve agreement to the experimental spectra in the case of **L3**. Initial geometry guess was generated using either crystallographic data molecular mechanics as implemented in Avogadro version 1.2.0 using the UFF force field [46]. Mean crystallographic planes were calculated using Mercury version 3.7.

5.3. Photophysical measurements

Steady-state emission spectra were recorded using a PTI QM-40 instrument with a PMT detector, which is sensitive up to 850 nm. Luminescence quantum yields were determined using [Ru (bipy)$_3$] Cl_2 (in aqueous solution) as a standard following known procedures; uncertainties are estimated at 20% or better [47–49]. The luminescence lifetimes of the complexes were measured by time-correlated single-photon counting following excitation with a 365, 405, or 450 nm LED in methylene chloride. All samples were de-gassed for 5 min.

5.4. X-ray diffraction

X-ray diffraction data were collected on a Bruker APEX 2 CCD platform diffractometer (Mo Ka (l = 0.71073 Å)) at 125 K with crystals mounted in a nylon loop with Paratone-N cryoprotectant oil. The structure of **O3** was solved using direct methods (SHELXS-97) and standard difference map techniques, and was refined by full-matrix least-squares procedures on F^2 with SHELXL-97 [50] **L3** was crystallized by slow diffusion of hexane into a chloroform solution in an NMR tube. The structure was solved using direct methods (SHELXT 2014/4) [51] and standard difference map techniques, and was refined by full-matrix least-squares procedures on F^2 with SHELXL-2016/6 [52]. All non-hydrogen atoms were refined anisotropically. Hydrogen atoms on carbon were included in calculated positions and were refined using a riding model. CELL_NOW (v2008/4) revealed that **L3** contained two twin domains. Both domains were integrated with SAINT (v8.34A) using the two-component orientation matrix produced by CELL_NOW. The data was scaled and absorption corrected with TWINABS (v2012/1). The initial solution was refined with single component data for the stronger domain before final refinement with an HKLF 5 dataset constructed from all observations involving domain 1. See Figs. 1 and 2 and the captions for ORTEP drawings, labels, bond lengths, and bond angles. CIF for compounds **O1** and **L3** is included in the supporting information.

5.5. Preparation of the compounds

Platinum dimer, cis-[Pt_2Me_4 (μ-SMe_2)$_2$], **PtA**, was prepared as reported elsewhere [53]. **L1** and **M1** were synthesized by adapting existing procedures [30,54–57].

[$C_{13}H_9NS$] (**L1**): 2-bromopyridine (0.3102 g, 1.96 mmol), benzo [*b*]thien-3-ylboronic acid (0.6989 g, 3.93 mmol), tetrakis-(triphenylphosphine)-palladium (0) (0.1202 g, 0.1040 mmol), and K_2CO_3 (0.8140 g, 5.89 mmol) were dissolved in degassed DMF (5 mL) and degassed H_2O (1.25 mL). The mixture was stirred for 4 h at 60 °C under argon. The resulting solution was extracted with ethyl acetate and the solvent was removed under vacuum. The desired compound was isolated by flash chromatography with 50% hexane and ethyl acetate as the eluents. The resulting product appeared as a pink oil. Yield 0.2166 g (1.03 mmol, 52%). ^{1}H NMR (400 MHz, $CDCl_3$) δ = 8.76 (d, *J* = 4.9 Hz, 1H), 8.46 (d, *J* = 8.1 Hz, 1H), 7.91 (d, *J* = 7.8 Hz, 1H), 7.80 (s, 1H), 7.78 (t, *J* = 7.8 Hz, 1H), 7.70 (d, *J* = 7.8 Hz, 1H), 7.45 (t, *J* = 7.6 Hz, 1H), 7.40 (t, *J* = 7.8 Hz, 1H), 7.28 (t, *J* = 4.9 Hz, 1H). ^{13}C NMR (100 MHz, $CDCl_3$) δ = 122.12, 122.74, 122.84, 124.21, 124.70, 124.80, 126.51, 136.75, 136.78, 137.35, 140.99, 149.77, 154.75.

[$C_{17}H_{11}NS$] (**M1**): 2-bromoquinoline (0.2137 g, 1.03 mmol), benzo [*b*]thien-3-ylboronic acid (0.3683 g, 2.06 mmol), tetrakis-(triphenylphosphine)-palladium (0) (0.0658 g, 0.0570 mmol), and K_2CO_3 (0.2858 g, 2.06 mmol) were dissolved in degassed DMF (1.4 mL) and degassed water (0.35 mL). The solution was stirred for 6 ½ hours at 60 °C under argon and a blue color was observed. The solution was extracted with dichloromethane and the solvent was removed under vacuum. The desired complex was isolated by flash chromatography using 50% hexane and ethyl acetate as the eluents. Yield: 0.2574 g (0.985 mmol, 96%).^{1}H NMR (400 MHz, $CDCl_3$): δ = 7.43 (d, ^{3}J = 8.0 Hz, 1H), 7.51 (d, ^{3}J = 7.8 Hz, 1H), 7.56 (t, ^{3}J = 7.5 Hz, 1H), 7.76 (t, ^{3}J = 7.5 Hz, 1H), 7.85 (d, ^{3}J = 8.3 Hz, 1H), 7.86 (d, ^{3}J = 7.6 Hz, 1H), 7.94 (d, ^{3}J = 7.9 Hz, 1H), 7.97 (s, 1H), 8.22 (d, ^{3}J = 8.6 Hz, 1H), 8.25 (d, ^{3}J = 8.7 Hz, 1H), 8.83 (d, ^{3}J = 8.0 Hz, 1H). ^{13}C

NMR (100 MHz, CDCl3): δ = 121.01, 122.78, 124.93, 125.00, 125.03, 126.56, 127.13, 127.68, 127.72, 129.75, 129.91, 136.76, 137.60, 137.46, 141.06, 148.24, 154.64.

[$C_{17}H_{11}NS$] (**O1**): 8-bromoquinoline (0.0757 g, 0.3638 mmol), benzo [*b*]thien-3-ylboronic acid (0.1303 g, 0.7313 mmol), tetrakis-(triphenylphosphine)-palladium (0) (0.0210 g, 0.0182 mmol), and K_2CO_3 (0.1534 g, 1.11 mmol) were dissolved in degassed DMF (5.00 mL) and degassed H_2O (1.25 mL). The solution was stirred at 60 °C for 6 ½ hours under argon. The solution was extracted with dichloromethane and the solvent was removed under vacuum. The desired complex was isolated by flash chromatography using 50% hexane and ethyl acetate as the eluents. A light pink solid was collected. Yield 0.0463 g (0.1772 mmol, 48%). ^{1}H NMR (400 MHz, $CDCl_3$): δ = 7.29 (t, 7.8 Hz, 1H), 7.36 (t, *J* = 7.4 Hz, 1H), 7.44 (dd, *J* = 8.1, 4.2 Hz, 1H), 7.51 (d, ^{3}J = 8.0 Hz, 1H), 7.64 (dd, ^{3}J = 7.2, 8.9 Hz, 1H) 7.65 (s, 1H), 7.85 (d, ^{3}J = 7.2 Hz, 1H), 7.90 (d, ^{3}J = 8.1 Hz, 1H), 7.94 (d, ^{3}J = 8.0 Hz, 1H), 8.25 (d, ^{3}J = 8.4 Hz, 1H), 8.90 (d, ^{3}J = 4.2 Hz, 1H). ^{13}C NMR (100 MHz, CDCl3): δ = 121.37, 122.84, 132.85, 124.05, 124.29, 125.99, 126.39, 128.16, 128.89, 131.22, 135.36, 135.38, 136.42, 139.51, 140.19, 146.85, 150.48.

[$C_{16}H_{17}NPtS_2$] (**L2**): **L1** (0.0147 g, 0.0696 mmol) and $Pt_2Me_4(SMe_2)_2$ (0.0200 g, 0.0348 mmol) were dissolved in dry toluene (5.00 mL). The solution was stirred under argon for 2 h at RT, followed by an hour stir at 60 °C under argon. The solvent was removed under vacuum yielding a yellow-orange solid. Yield 0.0281 g (0.0582 mmol, 84%). ^{1}H NMR (400 MHz, $CDCl_3$): δ = 1.23 (s, $^2J_{(Pt-H)}$ = 78.8 Hz, 3H), 2.51 (s, $^3J_{(Pt-H)}$ = 29.5 Hz, 6H), 7.12 (t, ^{3}J = 6.4 Hz, 1H), 7.21 (t, ^{3}J = 7.5 Hz, 1H), 7.34 (t, ^{3}J = 7.5 Hz, 1H), 7.86 (t, ^{3}J = 8.0 Hz, 1H), 7.89 (d, ^{3}J = 7.7 Hz, 1H), 8.00 (d, ^{3}J = 8.1 Hz, 1H), 8.07 (d, ^{3}J = 8.1 Hz, 1H), 8.78 (d, ^{3}J = 5.6 Hz, 1H). ^{13}C NMR (100 MHz, CDCl3): δ = 20.18, 23.55, 117.79, 118.34, 119.19, 120.15, 121.49, 122.40, 123.00, 123.17, 124.12, 124.95, 138.35, 146.38, 150.61. HR-ESI-(+)-MS: *m*/*z* 482.0492 calcd for $C_{16}H_{17}NPtS_2$; 482.0450.

[$C_{19}H_{17}NPtS$] (**O2'**): **O1** (0.0060 g, 0.023 mmol) and $Pt_2Me_4(SMe_2)_2$ (0.0088 g, 0.0015 mmol) were dissolved in dry toluene (5.00 mL). The solution was stirred at RT for 2 h under argon. The solvent was removed under vacuum. Yield: 7.8 mg (0.0016 mmol, 68%). ^{1}H NMR (400 MHz, $CDCl_3$): δ = −0.40 (s, $^2J_{(Pt-H)}$ = 81.4 Hz, 3H), 1.10 (s, $^2J_{(Pt-H)}$ = 88.3 Hz, 3H), 6.23 (s, $^2J_{(Pt-H)}$ = 50.6 Hz, 1H), 7.41 (t, ^{3}J = 7.3 Hz, 1H), 7.47 (t, ^{3}J = 7.3 Hz, 1H), 7.54 (t, ^{3}J = 7.6 Hz, 1H), 7.58 (dd, ^{3}J = 4.9, 8.5 Hz, 1H), 7.76 (t, ^{3}J = 8.9 Hz, 1H), 7.82 (d, ^{3}J = 7.9 Hz, 1H), 8.10 (d, ^{3}J = 7.7 Hz, 1H), 8.42 (d, ^{3}J = 8.4 Hz, 1H), 9.23 (d, ^{3}J = 4.9 Hz, $^3J_{(Pt-H)}$ = 22.0 Hz, 1H). ^{13}C NMR (100 MHz, CDCl3): δ = −10.33, 10.78, 29.37, 91.17, 122.42, 122.99, 123.29, 124.50, 124.90, 126.59, 126.84, 127.80, 130.63, 130.73, 137.00, 138.45, 143.55, 148.04, 149.70.

[$C_{20}H_{19}NPtS_2$] (**O2**): **O1** (0.0200 g, 0.0765 mmol) and $Pt_2Me_4(SMe_2)_2$ (0.0220 mg, 0.0383 mmol) were dissolved in dry toluene (5.00 mL). The solution was stirred at 60 °C for 2 h under argon. The solvent was removed under vacuum yielding a golden-orange solid. Yield: 0.0355 g (0.0667 mmol, 87%). ^{1}H NMR (400 MHz, $CDCl_3$): δ = 1.24 (s, $^2J_{(Pt-H)}$ = 81.0 Hz, 3H), 2.29 (s, $^3J_{(Pt-H)}$ = 27.7 Hz, 6H), 7.14 (t, 7.3 Hz, 1H), 7.18 (t, *J* = 7.3 Hz, 1H), 7.37 (dd, *J* = 5.0, 8.0 Hz, 1H), 7.68−7.73 (m, 2H) 7.84 (d, ^{3}J = 7.6 Hz, 1H), 7.95 (d, ^{3}J = 7.9 Hz, 1H), 8.37 (d, ^{3}J = 8.6 Hz, 1H), 8.40 (d, ^{3}J = 6.0 Hz, 1H), 9.29 (d, ^{3}J = 5.0 Hz, $^3J_{(Pt-H)}$ = 20.4 Hz, 1H). ^{13}C NMR (100 MHz, CDCl3): δ = 20.40, 110.15, 120.86, 121.12, 121.26, 122.34, 122.99, 123.34, 123.38, 124.71, 124.97, 127.56, 129.84, 130.06, 136.48, 138.65, 144.19, 152.18. NMR experimental monitoring: (4.3 mg, 0.016 mmol) mixed with Pt-Dimer (8.0 mg, 0.014 mmol) in dry toluene-d_8 (0.7 mL) in a J. Young NMR tube which was frozen in liquid nitrogen, purged, and thawed three times before being exposed to a N_2 atmosphere. The tube was then sealed and heated on an oil bath at 60 °C for a total of 150 min. Solvent removed, yielding a golden solid (9.6 mg, 65% yield). ^{1}H NMR (400 MHz, $CDCl_3$): δ = 1.24 [s, $^2J_{(Pt-H)}$ = 81.1 Hz, 3H, H^m]; 2.29 [s, $^3J_{(Pt-H)}$ = 27.4 Hz, 6H, H^l]; 7.14 [ddd, ^3J = 15.3 Hz, ^4J = 2.4 Hz, 1H, H^d]; 7.21 [ddd, ^3J = 15.3 Hz, ^4J = 2.4 Hz, 1H, H^c]; 7.36 [dd, ^3J = 8.0 Hz, ^4J = 4.9 Hz, 1H, H^j]; 7.71−7.72 [m, 2H, $H^{e/g}$]; 7.83 [d, ^3J = 7.6 Hz, 1H, H^f]; 7.95 [d, ^3J = 8.1 Hz, 1H, H^i]; 8.36 [dd, ^3J = 8.2 Hz, ^4J = 1.7 Hz, 1H, H^h]; 8.39 [dd, ^3J = 6.1 Hz, ^4J = 2.7 Hz, 1H, H^b]; 9.28 [dd, ^3J = 4.9 Hz, ^4J = 1.7 Hz, 1H, H^k].

[$C_{26}H_{16}N_2PtS_2$] (**L3**): **L1** (0.0587 g, 0.2778 mmol) and $Pt_2Me_4(SMe_2)_2$ (0.0468 g, 0.0815 mmol) were dissolved in dry toluene (4 mL). The solution was stirred under argon at 80 °C for 5 h, followed by a 1 h stir under blue light (450 nm). The solvent was removed under vacuum and a wash with dichloromethane was performed yielding a red solid. The precipitate was collected. Yield 0.0369 g (0.0599 mmol, 74%.). ^{1}H NMR (400 MHz, $CDCl_3$) δ = 8.63 (d, *J* = 6.0 Hz, $^3J_{(Pt-H)}$ = 22.0 Hz, 1H), 8.02 (d, *J* = 8.1 Hz, 1H), 7.88 (d, *J* = 7.9 Hz, 1H), 7.85 (d, *J* = 8.2 Hz, 1H), 7.70 (t, *J* = 7.8 Hz, 1H), 7.38 (t, *J* = 7.6 Hz, 1H), 7.25 (t, *J* = 7.2 Hz, 1H), 7.05 (t, *J* = 6.2 Hz, 1H). ^{1}H NMR (400 MHz, $(CD_3)_2SO$) δ = 8.92 (d, *J* = 5.7 Hz, 1H), 8.29−8.34 (m, 2H), 8.18 (t, *J* = 7.8 Hz, 1H), 8.02 (d, *J* = 7.9 Hz, 1H), 7.51 (t, *J* = 6.6 Hz, 1H), 7.43 (t, *J* = 7.7 Hz, 1H), 7.30 (t, *J* = 7.5 Hz, 1H). ^{13}C NMR (100 MHz, $CDCl_3$) δ = 162.06, 158.75, 148.42, 144.69, 139.40, 138.82, 136.77, 124.27, 122.62, 121.70, 119.25, 119.05, 118.09. HR-ESI-(+)-MS: *m*/*z* 615.0485 calcd for $C_{26}H_{16}N_2PtS_2$; 615.0403.

[$C_{34}H_{20}N_2PtS_2$] (**M3**): **M1** (0.0271 g, 0.1037 mmol) and $Pt_2Me_4(SMe_2)_2$ (0.0155 g, 0.0270 mmol) were dissolved in dry toluene (5 mL). The solution was stirred under argon for 45 min at RT, followed by a 4 h stir at 60 °C. The solution remained in an inert atmosphere and was then stirred for 12 h under blue light (405 nm). The precipitate was collected. Yield: 9.90 g (0.0138 mmol, 53%). ^{1}H NMR (400 MHz, $CDCl_3$): δ = 8.36 (ABq, 2H, $\Delta\delta_{AB}$ = 0.01, J_{AB} = 8.92 Hz), 8.31 (d, 1H, ^{3}J = 8.21 Hz), 7.98 (d, 1H, ^{3}J = 7.92 Hz), 7.78 (d, 1H, ^{3}J = 8.80 Hz), 7.72 (d, 1H, ^{3}J = 7.89 Hz), 7.46 (t, 1H, ^{3}J = 7.36 Hz), 7.31 (t, 1H, ^{3}J = 7.49 Hz), 7.20 (t, 1H, ^{3}J = 7.27 Hz), 6.81 (t, 1H, ^{3}J = 7.44 Hz). ^{1}H NMR (400 MHz, $(CD_3)_2SO$): δ = 8.75 (d, 1H, ^3J = 8.75 Hz), 8.61 (d, 1H, ^{3}J = 8.91 Hz), 8.55 (d, 1H, ^{3}J = 8.03 Hz), 8.10 (d, 1H, ^{3}J = 7.94 Hz), 8.02 (d, 1H, ^{3}J = 8.12 Hz), 7.65 (d, 1H, ^{3}J = 8.69 Hz), 7.52 (t, 1H, ^{3}J = 7.47 Hz), 7.38 (t, 1H, ^{3}J = 7.55 Hz), 7.34 (t, 1H, ^{3}J = 7.55 Hz), 6.92 (t, 1H, ^{3}J = 7.55 Hz). ^{13}C NMR (100 MHz, $(CD_3)_2SO$): δ = 162.77, 161.75, 147.10, 143.38, 141.09, 140.70, 136.48, 129.41, 128.33, 126.31, 125.55, 125.18, 124.89, 122.69, 122.49, 119.90, 117.43. HR-ESI-(+)-MS: *m*/*z* 715.0792 calcd for $C_{34}H_{20}N_2PtS_2$; 715.0716.

Notes

The authors declare no competing financial interest.

Acknowledgments

This material is based upon work supported by the US National Science Foundation under CHE-1665435 (Craig M. Anderson (CMA), P.I.). We also thank Bard Summer Research Institute (BSRI) for support. Mass spectrometry was run at Vassar College with the help of Prof. Teresa Garrett. We thank Prof. Christopher LaFratta for help obtaining photophysical data.

Appendix A. Supplementary data

Supplementary data to this article can be found online at https://doi.org/10.1016/j.jorganchem.2018.12.010.

References

[1] C. Lentz, O. Schott, T. Auvray, G. Hanan, B. Elias, Photocatalytic hydrogen production using a red-absorbing Ir(III)−Co(III) dyad, Inorg. Chem. 56 (2017)

10875–10881, https://doi.org/10.1021/acs.inorgchem.7b00684.
[2] T. Fleetham, G. Li, J. Li, Phosphorescent Pt(II) and Pd(II) complexes for efficient, high-color-quality, and stable OLEDs, Adv. Mater. 29 (2016) 1601861, https://doi.org/10.1002/adma.201601861.
[3] S. Jamali, S.M. Nabavizadeh, M. Rashidi, Binuclear cyclometalated organoplatinum complexes containing 1,1′-Bis(diphenylphosphino)ferrocene as spacer ligand: kinetics and mechanism of MeI oxidative addition, Inorg. Chem. 47 (2008) 5441–5452, https://doi.org/10.1021/ic701910d.
[4] J.H. Alstrum-Acevedo, M.K. Brennaman, T.J. Meyer, Chemical approaches to artificial photosynthesis. 2, Inorg. Chem. 44 (2005) 6802–6827, https://doi.org/10.1021/ic050904r.
[5] J. Boixel, V. Guerchais, H. Le Bozec, D. Jacquemin, A. Amar, A. Boucekkine, et al., Second-order NLO switches from molecules to polymer films based on photochromic cyclometalated platinum(II) complexes, J. Am. Chem. Soc. 136 (2014) 5367–5375, https://doi.org/10.1021/ja4131615.
[6] J. Kalinowski, V. Fattori, M. Cocchi, J.A.G. Williams, Light-emitting devices based on organometallic platinum complexes as emitters, Coord. Chem. Rev. 255 (2011) 2401–2425, https://doi.org/10.1016/j.ccr.2011.01.049.
[7] I. Omae, Application of the five-membered ring blue light-emitting iridium products of cyclometalation reactions, as OLEDs, Coord. Chem. Rev. (2015) 1–72, https://doi.org/10.1016/j.ccr.2015.08.009.
[8] H. Xu, R. Chen, Q. Sun, W. Lai, Q. Su, W. Huang, et al., Recent progress in metal–organic complexes for optoelectronic applications, Chem. Soc. Rev. 43 (2014) 3259–3302, https://doi.org/10.1039/C3CS60449G.
[9] C.M. Anderson, M.A. Weinstein, J. Morris, N. Kfoury, L. Duman, T.A. Balema, et al., Biscyclometalated platinum complexes with thiophene ligands, J. Organomet. Chem. 723 (2013) 188–197, https://doi.org/10.1016/j.jorganchem.2012.10.027.
[10] L.M. Rendina, R.P.C. reviews, Oxidative addition reactions of organoplatinum (II) complexes with nitrogen-donor ligands, ACS Publications 97 (1997) (1997) 1735–1754, https://doi.org/10.1021/cr9704671.
[11] M. Albrecht, Cyclometalation using d-block transition metals: fundamental aspects and recent trends, Chem. Rev. 110 (2010) 576–623, https://doi.org/10.1021/cr900279a.
[12] E.G. Bowes, S. Pal, J.A. Love, Exclusive csp 3–csp 3vs csp 2–csp 3 Reductive elimination from Pt IVGoverned by ligand constraints, J. Am. Chem. Soc. 137 (2015) 16004–16007, https://doi.org/10.1021/jacs.5b10993.
[13] S. Lentijo, J.A. Miguel, P. Espinet, Cyclopalladated complexes of perylene imine: formation of acetato-bridged dinuclear complexes with 6,6- and 5,6-membered metallacycles, Organometallics 30 (2011) 1059–1066, https://doi.org/10.1021/om1010929.
[14] L. Keyes, T. Wang, B.O. Patrick, J.A. Love, Pt mediated Câ€"H activation: formation of a six membered platinacycle via Csp 3-H activation, Inorg. Chim. Acta. 380 (2012) 284–290, https://doi.org/10.1016/j.ica.2011.09.030.
[15] C.M. Anderson, M.W. Greenberg, L. Spano, L. Servatius, J.M. Tanski, Regioselective competition between the formation of seven-membered and five-membered cyclometalated platinacycles preceded by Csp2Csp 3 reductive elimination, J. Organomet. Chem. 819 (2016) 27–36, https://doi.org/10.1016/j.jorganchem.2016.06.018.
[16] S. Lentijo, J.A. Miguel, P. Espinet, Cyclopalladated complexes of perylene imine: formation of acetato-bridged dinuclear complexes with 6,6- and 5,6-membered metallacycles, Organometallics 30 (2011) 1059–1066, https://doi.org/10.1021/om1010929.
[17] A.R.B. Rao, S. Pal, Regioselective cyclometallation with some platinum group metal ions, J. Organomet. Chem. 762 (2014) 58–66, https://doi.org/10.1016/j.jorganchem.2014.04.009.
[18] R. Martín, M. Crespo, M. Font-Bardia, T. Calvet, Five- and seven-membered metallacycles in [C,N,N′] and [C,N] cycloplatinated compounds, Organometallics 28 (2009) 587–597, https://doi.org/10.1021/om800864f.
[19] M. Crespo, M. Font-Bardia, X. Solans, Compound [PtPh 2(SMe 2) 2] as a versatile metalating agent in the preparation of new types of [C,N,N'] cyclometalated platinum compounds, Organometallics 23 (2004) 1708–1713, https://doi.org/10.1021/om030674t.
[20] M. Crespo, M. Font-Bardia, T. Calvet, Biaryl formation in the synthesis of endo and exo-platinacycles, Dalton Trans. 40 (2011) 9431–9438, https://doi.org/10.1039/c1dt10664c.
[21] M. Crespo, E. Evangelio, Five- and six-membered platinacycles derived from phenantryl and anthracenyl imines, J. Organomet. Chem. 689 (2004) 1956–1964, https://doi.org/10.1016/j.jorganchem.2004.03.020.
[22] M. Crespo, M. Font-Bardia, X. Solans, Synthesis, reactivity and crystal structures of platinum (II) and platinum (IV) cyclometallated compounds derived from 2- and 4-biphenylimines, J. Organomet. Chem. 691 (2006) 444–454, https://doi.org/10.1016/j.jorganchem.2005.09.011.
[23] S. Kim, N. Dahal, T. Kesharwani, Environmentally benign process for the synthesis of 2,3-disubstituted benzo[b]thiophenes using electrophilic cyclization, Tetrahedron Lett. 54 (2013) 4373–4376, https://doi.org/10.1016/j.tetlet.2013.05.139.
[24] T. Kesharwani, C.T. Kornman, A.L. Tonnaer, A.D. Royappa, Green synthesis of benzo[b]thiophenes via iron(III) mediated 5-endo-dig iodocyclization of 2-alkynylthioanisoles, Tetrahedron Lett. 57 (2016) 411–414, https://doi.org/10.1016/j.tetlet.2015.12.037.
[25] T. Kesharwani, K.A. Giraudy, J.L. Morgan, C. Kornman, A.D. Olaitan, Green synthesis of halogenated thiophenes, selenophenes and benzo[b]selenophenes using sodium halides as a source of electrophilic halogens, Tetrahedron Lett. 58 (2017) 638–641, https://doi.org/10.1016/j.tetlet.2017.01.007.
[26] T. Kesharwani, J. Craig, C. Del Rosario, R. Shavnore, C. Kornman, Synthesis of 3-iodobenzo[b]thiophenes via iodocyclization/etherification reaction sequence, Tetrahedron Lett. 55 (2014) 6812–6816, https://doi.org/10.1016/j.tetlet.2014.10.064.
[27] M.S. Khan, M.K. Al-Suti, J. Maharaja, A. Haque, R. Al-Balushi, P.R. Raithby, Conjugated poly-ynes and poly(metalla-ynes) incorporating thiophene-based spacers for solar cell (SC) applications, J. Organomet. Chem. 812 (2016) 13–33, https://doi.org/10.1016/j.jorganchem.2015.10.003.
[28] C.M. Anderson, M. Crespo, J.M. Tanski, Synthesis and reactivity of coordination and six-membered, cyclometalated platinum complexes containing a bulky diimine ligand, Organometallics 29 (2010) 2676–2684, https://doi.org/10.1021/om100068j.
[29] V.N. Kozhevnikov, M.C. Durrant, J.A.G. Williams, Highly luminescent mixed-metal Pt(II)/Ir(III) complexes: bis-cyclometalation of 4,6-diphenylpyrimidine as a versatile route to rigid multimetallic assemblies, Inorg. Chem. 50 (2011) 6304–6313, https://doi.org/10.1021/ic200706e.
[30] V.V. Sivchik, A.I. Solomatina, Y.-T. Chen, A.J. Karttunen, S.P. Tunik, P.-T. Chou, et al., Halogen bonding to amplify luminescence: a case study using a platinum cyclometalated complex, Angew. Chem. 127 (2015) 14263–14266, https://doi.org/10.1002/ange.201507229.
[31] E.A. Medlycott, G.S. Hanan, Designing tridentate ligands for ruthenium(ii) complexes with prolonged room temperature luminescence lifetimes, Chem. Soc. Rev. 34 (2005), https://doi.org/10.1039/b316486c, 133–11.
[32] D.N. Kozhevnikov, V.N. Kozhevnikov, M.Z. Shafikov, A.M. Prokhorov, D.W. Bruce, J.A. Gareth Williams, Phosphorescence vs fluorescence in cyclometalated platinum(II) and iridium(III) complexes of (Oligo)thienylpyridines, Inorg. Chem. 50 (2011) 3804–3815, https://doi.org/10.1021/ic200210e.
[33] R. Tan, D. Song, C–H and C–S activations of quinoline-functionalized thiophenes by platinum complexes, Organometallics 30 (2011) 1637–1645, https://doi.org/10.1021/om101171s.
[34] R. Tan, D. Song, Platinum complexes of η 2-thiophenes, Inorg. Chem. 49 (2010) 2026–2028, https://doi.org/10.1021/ic902289h.
[35] C.M. Anderson, M.W. Greenberg, T.A. Balema, L.M. Duman, N. Oh, A. Hashmi, et al., Regioselective formation of six-membered platinacycles by Câ€"X and Câ€"H oxidative addition, Tetrahedron Lett. 56 (2015) 6352–6355, https://doi.org/10.1016/j.tetlet.2015.09.121.
[36] C.M. Anderson, N. Oh, T.A. Balema, F. Mastrocinque, C. Mastrocinque, D. Santos, et al., Regioselective Câ€"H/Câ€"X activation of naphthyl-derived ligands to form six-membered palladacycles, Tetrahedron Lett. 57 (2016) 4574–4577, https://doi.org/10.1016/j.tetlet.2016.08.092.
[37] C.M. Anderson, M. Crespo, M.C. Jennings, A.J. Lough, G. Ferguson, R.J. Puddephatt, Competition between intramolecular oxidative addition and ortho metalation in organoplatinum(II) compounds: activation of aryl-halogen bonds, Organometallics 10 (1991) 2672–2679, https://doi.org/10.1021/om00054a031.
[38] T. Okada, I.M. El-Mehasseb, M. Kodaka, T. Tomohiro, K.-I. Okamoto, H. Okuno, Mononuclear platinum(II) complex with 2-phenylpyridine ligands showing high cytotoxicity against mouse sarcoma 180 cells acquiring high cisplatin resistance, J. Med. Chem. 44 (2001) 4661–4667, https://doi.org/10.1021/jm010203d.
[39] F. Juliá, P. González-Herrero, Aromatic C–H activation in the triplet excited state of cyclometalated platinum(II) complexes using visible light, J. Am. Chem. Soc. 138 (2016) 5276–5282, https://doi.org/10.1021/jacs.5b13311.
[40] M. Bachmann, D. Suter, O. Blacque, K. Venkatesan, Tunable and efficient white light phosphorescent emission based on single component N-heterocyclic carbene platinum(II) complexes, Inorg. Chem. 55 (2016) 4733–4745, https://doi.org/10.1021/acs.inorgchem.5b02962.
[41] R.L. Martin, Natural transition orbitals, J. Chem. Phys. 118 (2003) 4775–4777, https://doi.org/10.1063/1.1558471.
[42] L. Zhang, L. Tian, M. Li, R. He, W. Shen, A theoretical study on tuning the electronic structures and photophysical properties of newly designed platinum(ii) complexes by adding substituents on functionalized ligands as highly efficient OLED emitters, Dalton Trans. 43 (2014) 6500–6512, https://doi.org/10.1039/C3DT53209G.
[43] S. Gauthier, B. Caro, F. Robin-Le Guen, N. Bhuvanesh, J.A. Gladysz, L. Wojcik, et al., Synthesis, photovoltaic performances and TD-DFT modeling of push–pull diacetylide platinum complexes in TiO 2 based dye-sensitized solar cells, Dalton Trans. 43 (2014) 11233–11242, https://doi.org/10.1039/C4DT00301B.
[44] R. Liu, A. Azenkeng, Y. Li, W. Sun, Long-lived platinum(ii) diimine complexes with broadband excited-state absorption: efficient nonlinear absorbing materials, Dalton Trans. 41 (2012) 12353–12357, https://doi.org/10.1039/c2dt31267k.
[45] A.D. Bochevarov, E. Harder, T.F. Hughes, J.R. Greenwood, D.A. Braden, D.M. Philipp, et al., Jaguar: a high-performance quantum chemistry software program with strengths in life and materials sciences, Int. J. Quant. Chem. 113 (2013) 2110–2142, https://doi.org/10.1002/qua.24481.
[46] M.D. Hanwell, D.E. Curtis, D.C. Lonie, T. Vandermeersch, E. Zurek, G.R. Hutchison, Avogadro: an advanced semantic chemical editor, visualization, and analysis platform, J. Cheminf. 4 (2012) 1, https://doi.org/10.1186/1758-2946-4-17, 4 (2012) 17.
[47] G.F. Manbeck, W.W. Brennessel, R. Eisenberg, Photoluminescent copper(I) complexes with amido-triazolato ligands, Inorg. Chem. 50 (2011) 3431–3441, https://doi.org/10.1021/ic102338g.
[48] D.N. Kozhevnikov, V.N. Kozhevnikov, M.Z. Shafikov, A.M. Prokhorov, D.W. Bruce, J.A. Gareth Williams, Phosphorescence vs fluorescence in

cyclometalated platinum(II) and iridium(III) complexes of (Oligo)thienylpyridines, Inorg. Chem. 50 (2011) 3804–3815, https://doi.org/10.1021/ic200210e.
[49] J. Van Houten, R.J. Watts, Temperature dependence of the photophysical and photochemical properties of the tris(2,2'-bipyridyl)ruthenium(II) ion in aqueous solution, J. Am. Chem. Soc. 98 (1976) 4853–4858, https://doi.org/10.1021/ja00432a028.
[50] G.M. Sheldrick, A short history of SHELX, Acta Crystallogr a Found Crystallogr 64 (2007) 112–122, https://doi.org/10.1107/S0108767307043930.
[51] G.M. Sheldrick, SHELXT – integrated space-group and crystal- structure determination, Acta Crystallogr. A71 (2015) 3–8, https://doi.org/10.1107/S2053273314026370 (2015) 1–6. doi:10.1107/S2053273314026370.
[52] G.M. Sheldrick, Crystal structure refinement with SHELXL, Acta Crystallogr. C71 (2015) 3–8, https://doi.org/10.1107/S2053229614024218 (2015) 1–6. doi:10.1107/S2053229614024218.
[53] J.D. Scott, R.J. Puddephatt, Ligand dissociation as a preliminary step in methyl-for-halogen exchange reactions of platinum(II) complexes, Organometallics 2 (2002) 1643–1648, https://doi.org/10.1021/om50005a028.
[54] B. Qu, H.P.R. Mangunuru, S. Tcyrulnikov, D. Rivalti, O.V. Zatolochnaya, D. Kurouski, et al., Enantioselective synthesis of α-(hetero)aryl piperidines through asymmetric hydrogenation of pyridinium salts and its mechanistic insights, Org. Lett. 20 (2018) 1333–1337, https://doi.org/10.1021/acs.orglett.8b00067.
[55] Y. Zou, G. Yue, J. Xu, J.S. Zhou, General Suzuki coupling of heteroaryl bromides by using tri- tert-butylphosphine as a supporting ligand, Eur. J. Org. Chem. 2014 (2014) 5901–5905, https://doi.org/10.1002/ejoc.201402915.
[56] J. Yang, S. Liu, J.-F. Zheng, J.S. Zhou, Room-Temperature suzuki-miyaura coupling of heteroaryl chlorides and tosylates, Eur. J. Org. Chem. 2012 (2012) 6248–6259, https://doi.org/10.1002/ejoc.201200918.
[57] F.-F. Zhuo, W.-W. Xie, Y.-X. Yang, L. Zhang, P. Wang, R. Yuan, et al., TMEDA-assisted effective direct ortho arylation of electron-deficient N-heteroarenes with aromatic grignard reagents, J. Org. Chem. 78 (2013) 3243–3249, https://doi.org/10.1021/jo400152f.